



# Various mechanisms for double capture from helium targets by alpha particles

Dževad Belkić<sup>1,2</sup>

Received: 6 July 2023 / Accepted: 20 July 2023 / Published online: 9 August 2023  
© The Author(s) 2023

## Abstract

An analysis is presented using six quantum-mechanical four-body distorted wave (DW) theories for double capture (DC) in ion-atom collisions at intermediate and high energies. They all satisfy the correct boundary conditions in the entrance and exit channels. This implies the usage of short-range perturbation potentials in compliance with the exact behaviors of scattering wave functions at infinitely large separations of particles. Specifically, total cross sections  $Q$  are analyzed for collisions of alpha particles with helium targets. Regarding the relative quantitative performance of the studied DW theories at different impact energies  $E$ , our main focus is on the sensitivity of  $Q$  to various collisional mechanisms. The usual mechanism in most DW theories assumes that both electrons undergo the same type of collisions with nuclei. These are either single or double collisions in one or two steps, respectively, per channel, but without their mixture in either channel. The signatures of double collisions in differential cross sections are the Thomas peaks. By definition, these cannot be produced by single collisions. There is another DC pathway, which is actually favored by the existing experimental data. It is a hybrid, two-center mechanism which, in each channel separately, combines a single collision for one electron with a double collision for the other electron. The ensuing DW theory is called the four-body single-double scattering (SDS-4B) method. It appears that this mechanism in the SDS-4B method is more probable than double collisions for each electron in both channels predicted by the four-body continuum distorted wave (CDW-4B) method. This is presently demonstrated for  $Q$  at energies  $E=[200,8000]$  keV in DC exemplified by alpha particles colliding with helium targets.

---

✉ Dževad Belkić  
dzevad.belkic@ki.se

<sup>1</sup> Department of Oncology-Pathology, Karolinska Institute, P.O. Box 260, 171 76 Stockholm, Sweden

<sup>2</sup> Radiation Physics and Nuclear Medicine, Karolinska University Hospital, P.O. Box 260, 171 76 Stockholm, Sweden

**Keywords** Double charge exchange · Correct boundary conditions · Distorted wave theories

## 1 Introduction

This study is on several quantum-mechanical four-body perturbative distorted wave (DW) theories with correct boundary conditions. The present applications deal with total cross sections  $Q$  for double capture (DC) by alpha particles from helium targets. For a long time now, this process at intermediate and high energies  $E$  persists to be elusive and ineffable by the lowest-order of the Dodd-Greider perturbation series expansion [1], despite the absence of divergent disconnected diagrams. Various DW choices for DC for the studied problem yield the values of  $Q$  that unexpectedly deviate even by 1–3 orders of magnitude from the experimental data above 200 keV. This runs contrary to the well-documented reliability of these theories on  $Q$  in single capture (SC) for the same colliding particles [2–8].

A legitimate question then to ask is: should such a discouraging status disqualify the perturbative DW theories for  $Q$  in DC? The answer is in the negative. The stated failure to quantitatively reproduce the experimental data on  $Q$  in DC at all  $E$  above 200 keV is not universal, as it occurs in some, but not in all the mechanisms. The unsatisfactory mechanisms operating in the entrance and exit channels are with a single-step DC for both electrons, as in the four-body boundary corrected first Born (CB1-4B) method [9, 10]. The same holds true with a two-step DC for both electrons, as in the four-body continuum distorted wave (CDW-4B) method [11, 12]. Much better performance above about 550 keV is for the mixed mechanisms with a one-step DC in one channel accompanied by a two-step DC in the other channel, as in the four-body boundary-corrected continuum intermediate state (BCIS-4B) method [13] and in the four-body Born distorted (BDW-4B) method [14, 15].

The least adequate for DC is the four-body continuum distorted wave eikonal initial state (CDW-EIS-4B) method [16, 17] because of crudely approximating the two electronic full Coulomb waves in the entrance channel by their asymptotic eikonal phases. The most favored by measurements is the single-double scattering (SDS-4B) method [18]. While preserving the correct boundary conditions in both the entrance and exit channels, this symmetrized two-center theory adopts a single-step DC for one electron and a double-step DC for the other electron.

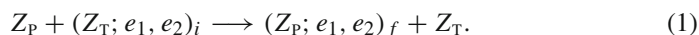
Destructive interference of heavy oscillations of electronic full Coulomb waves for continuum intermediate states is prone to cause notable reductions in  $Q$ . Four such waves appear in the CDW-4B method for DC. However, the CDW-4B method largely underestimates most of the measured total cross sections  $Q$  [19, 20]. On the other hand, the SDS-4B method includes two electronic full Coulomb waves (one per scattering center). It has been shown in Ref. [18] that the SDS-4B method for DC agrees excellently with the majority of the experimental data at energies above 200 keV. Supporting evidence for a more detailed relative performance of the SDS-4B and CDW-4B theories is illustrated in the present work by comparisons with all the available measurements on  $Q$ .

Further analyzed is a close relationship between the SDS-4B method for DC and the CDW-4B method for SC. In the latter theory for SC, an extra pathway to capture of the active electron is provided by the Coulomb interaction between the projectile nucleus and the passive electron. The same potential appears also in the perturbation interaction from the prior transition amplitude of the SDS-4B method for DC. It is therefore of interest to presently compare the relative contributions and energy dependence of this particular mode of electron capture.

Atomic units will be used throughout unless otherwise noted.

## 2 Theory

In considering DC for a collision of a bare nucleus with a heliumlike atomic target in its ground singlet state ( $1s^2 : ^1S$ ), the non-relativistic, non-radiative, spin-independent formalism is employed with two distinguishable electrons. In the entrance channel, a heavy bare nucleus P of charge  $Z_P$  and mass  $M_P \gg 1$  impacts upon a two-electron target containing a heavy nucleus T of charge  $Z_T$  and mass  $M_T \gg 1$ . In the exit channel, a new two-electron heliumlike atomic system is formed through DC containing P,  $e_1$  as well as  $e_2$ , while leaving behind the target remainder, the bare nucleus  $Z_T$ . Thus, initially,  $e_1$  and  $e_2$  move in the target atom in its stationary state. Finally, after collision, both target electrons are captured by P. As such, this scattering event is schematically represented by the following process:



The bound states of  $e_1$  and  $e_2$  are symbolized by the parentheses, where the subscripts  $i$  and  $f$  respectively refer to the standard sets of the initial and final quantum numbers. We denote by  $\mathbf{x}_k$  and  $\mathbf{s}_k$  the vectors connecting the  $k$ th electron  $e_k$  to T and P, respectively ( $k = 1, 2$ ). They define the inter-electronic vector  $\mathbf{x}_{12} = \mathbf{x}_1 - \mathbf{x}_2$  or  $\mathbf{s}_{12} = \mathbf{s}_1 - \mathbf{s}_2$ , where  $\mathbf{x}_{12} = \mathbf{s}_{12}$ . Further,  $\mathbf{R}$  is the vector connecting P and T (it relates to  $\mathbf{x}_k$  and  $\mathbf{s}_k$  via  $\mathbf{R} = \mathbf{x}_1 - \mathbf{s}_1 = \mathbf{x}_2 - \mathbf{s}_2$ ). Vector  $\mathbf{R}$  is resolved into its two components,  $\mathbf{R} = \boldsymbol{\rho} + \mathbf{v}Z$ , where  $\boldsymbol{\rho}$  is a two-dimensional vector in the scattering (XOY) plane and  $\mathbf{v}Z$  is along the Z-axis in the Galilean XOYZ reference system. The velocity vector  $\mathbf{v}$  of P (with the target at rest) is along the Z-axis. Vector  $\boldsymbol{\rho}$  should not be confused with the impact parameter  $\mathbf{b}$ , as we are not using the impact parameter method (IPM).

The initial and final bound-state wave functions, labeled by  $\varphi_i^T(\mathbf{x}_1, \mathbf{x}_2)$  and  $\varphi_f^P(\mathbf{s}_1, \mathbf{s}_2)$ , are associated with the binding energies  $E_i^T$  and  $E_f^P$ , respectively. The unperturbed (undistorted) entrance channel state  $\Phi_i$  is the product of  $\varphi_i^T$  and the plane wave for the free relative motion of  $Z_P$  and  $(Z_T; e_1, e_2)_i$ . Likewise, the unperturbed exit channel state  $\Phi_f$  is the product of  $\varphi_f^P$  and the plane wave for the free relative motion of  $(Z_P; e_1, e_2)_f$  and  $Z_T$ . In the DW theories,  $\Phi_i$  is distorted by the correlation effects between  $Z_P$  and  $(Z_T; e_1, e_2)_i$ . Similarly,  $\Phi_f$  is distorted by the correlation effects between  $(Z_P; e_1, e_2)_f$  and  $Z_T$ .

These dynamic correlation effects between P and  $(T, 2e)_i$  in the entrance channel as well as between T and  $(P, 2e)_f$  in the exit channel are described by the compound Coulomb distortions  $D_{i,f}^\pm$  in the distorted waves  $\chi_{i,f}^\pm$ . Here, the  $\pm$  signs refer to the

outgoing/incoming boundary conditions at large distances of particles, respectively. The forms of  $D_{i,f}^{\pm}$  depend on the descriptions of the motions of the electrons and heavy particles. Such distortions refer to the pairwise Coulomb interactions,  $P - e_{1,2}$  in the entrance channel,  $T - e_{1,2}$  in the exit channel as well as  $P$ - $T$  in both channels. Distorted waves  $\chi_{i,f}^{\pm}$  are the products of  $\Phi_{i,f}$  and  $D_{i,f}^{\pm}$  as  $\chi_{i,f}^{\pm} = \Phi_{i,f} D_{i,f}^{\pm}$ .

The electronic distorting factors in  $D_{i,f}^{\pm}$  are always placed on the nuclear center to which the electrons are not bound. Different choices of  $D_{i,f}^{\pm}$  give different DW methods. Thus, in the CDW-4B method for DC [11], the Coulomb distortion factors  $D_{i,f}^{\pm}$  are the products of the three full Coulomb wave functions. In this DW theory,  $D_i^+$  contains the two  $s_{1,2}$ -dependent electronic full Coulomb waves for  $e_{1,2}$  centered on  $Z_P$  (attractive potentials  $Z_P - e_{1,2}$ ). Likewise,  $D_f^-$  incorporates the two  $x_{1,2}$ -dependent electronic full Coulomb waves for  $e_{1,2}$  centered on  $Z_T$  (attractive potentials  $Z_T - e_{1,2}$ ).

The third Coulomb distortion per channel in the CDW-4B method is the full Coulomb wave due to the repulsive internuclear potential  $Z_P - Z_T$ , i.e.  $V_{PT} = Z_P Z_T / R$ . In this method, the product of two such waves appears in the transition amplitudes. However, in the limit  $1/M_{P,T} \ll 1$ , the ensuing  $R$ -dependent full Coulomb wave for the relative motion of heavy nuclei  $P$  and  $T$  can be replaced by its logarithmic Coulomb phase with a negligible error of the order of or less than  $1/\mu$ , where  $\mu$  is the reduced mass  $\mu = M_P M_T / (M_P + M_T)$ .

The product of such two phases gives a single phase  $(\mu\rho v)^{2iZ_P Z_T/v}$ , which contributes nothing to either the prior or post total cross sections  $Q_{if}^-$  or  $Q_{if}^+$ , respectively [2, 11, 18]. Therefore, for computations of  $Q_{if}^{\mp}$  in the CDW-4B method, this phase can be omitted from  $T_{if}^{\mp}$  and similarly in the CDW-EIS-4B method. Some other DW theories can contain the  $\rho$ -dependent phases, associated with the product of the Coulomb waves of heavy particles moving in the field of the screened nuclear charges of  $P$  and  $T$ . Such phases would not contribute either to  $Q_{if}^{\mp}$  and, thus, they too can be dropped from the pertinent transition amplitudes, as will presently be done.

The parts of the electronic full Coulomb waves (and their asymptotes) that distort the unperturbed channel states  $\Phi_{i,f}$  are written as:

$$\left. \begin{aligned} D_P^+(s_k) &= N^+(v_P) {}_1F_1(iv_P, 1, ivs_k + i\mathbf{v} \cdot \mathbf{s}_k); \quad k = 1, 2 \\ D_T^-(\mathbf{x}_k) &= N^-(v_T) {}_1F_1(-iv_T, 1, -ivx_k - i\mathbf{v} \cdot \mathbf{x}_k); \quad k = 1, 2 \\ D_P^+(s_1, s_2) &= \prod_{k=1}^2 D_P^+(s_k), \quad D_{P,\text{eik}}^+(s_1, s_2) = \prod_{k=1}^2 (vs_k + \mathbf{v} \cdot \mathbf{s}_k)^{-iv_P} \\ D_T^-(\mathbf{x}_1, \mathbf{x}_2) &= \prod_{k=1}^2 D_T^-(\mathbf{x}_k), \quad D_{T,\text{eik}}^-(\mathbf{x}_1, \mathbf{x}_2) = \prod_{k=1}^2 (vx_k + \mathbf{v} \cdot \mathbf{x}_k)^{iv_T} \\ N^{\pm}(v_K) &= e^{\pi v_K/2} \Gamma(1 \mp iv_K), \quad v_K = \frac{Z_K}{v} \quad (K = P, T) \end{aligned} \right\}. \quad (2)$$

The standard symbols  ${}_1F_1(a, b, z)$  and  $\Gamma(z)$  denote the Kummer function (i.e. the Gauss confluent hypergeometric function) and the Euler gamma function, respectively. In the Coulomb normalization constants  $N^{\pm}(v_K)$ , quantity  $v_K$  is the usual Sommerfeld parameter (also known as the perturbation parameter or the Coulomb interaction parameter).

In all the DW transition amplitudes, the product of the plane waves from the initial and the conjugated final state is contained in the standard exponential term  $\mathcal{E}_{dc}$ , which in the mass limit  $1/M_{p,T} \ll 1$ , acquires the form:

$$\mathcal{E}_{dc} = e^{i\alpha_{dc} \cdot (s_1 + s_2) + i\beta_{dc} \cdot (x_1 + x_2)}. \quad (3)$$

Vectors  $\alpha_{dc}$  and  $\beta_{dc}$  are comprised of the transverse momentum transfer  $\eta$  (the transverse or perpendicular component of the momentum transfer), the energy defect (difference between the initial and final bound-state energies) and the electron transition factors ( $\pm v/2$  per electron) as:

$$\left. \begin{aligned} \alpha_{dc} &= \frac{\eta - v_{dc}^+ v}{2}, \quad \beta_{dc} = -\frac{\eta + v_{dc}^- v}{2}, \quad \alpha_{dc} + \beta_{dc} = -v \\ v_{dc}^\pm &= 1 \pm \frac{\Delta E_{dc}}{v^2}, \quad \Delta E_{dc} = E_f^p - E_i^T \end{aligned} \right\}. \quad (4)$$

This is a succinct summary of the common, salient features of the DW methods for DC. We will now list the main working formulae of all the methods employed in Section 3. Because of their similarity, the first given will be transition amplitudes in the SDS-4B method for DC [18] and the CDW-4B method for SC [21]. Subsequently, provided will be transition amplitudes in the CB1-4B [9, 10], CDW-4B [11, 12], CDW-EIS-4B [16, 17], BCIS-4B [13] and BDW-4B [14, 15] methods. As noted, none of these transition amplitudes  $T_{if}^\mp$  will contain the discussed  $\rho$ -dependent phases factors because they do not contribute to  $Q_{if}^\mp$ .

## 2.1 The SDS-4B method (prior and post) for DC

$$\begin{aligned} T_{if,dc}^{(SDS-4B)-}(\eta) &= \iiint dx_1 dx_2 dR \mathcal{E}_{dc}(vR - v \cdot R)^{i\xi} \\ &\times \varphi_f^{p*}(s_1, s_2) \frac{1 + P_{12}}{\sqrt{2}} D_T^{-*}(x_1) V_{i,dc}^{(SDS-4B)} \varphi_i^T(x_1, x_2) D_P^+(s_1), \end{aligned} \quad (5)$$

$$\begin{aligned} T_{if,dc}^{(SDS-4B)+}(\eta) &= \iiint ds_1 ds_2 dR \mathcal{E}_{dc}(vR + v \cdot R)^{-i\xi} \\ &\times \varphi_i^T(x_1, x_2) \frac{1 + P_{12}}{\sqrt{2}} D_P^+(s_1) V_{f,dc}^{(SDS-4B)} \varphi_f^{p*}(s_1, s_2) D_T^{-*}(x_1), \end{aligned} \quad (6)$$

$$\left. \begin{aligned} V_{i,dc}^{(SDS-4B)} &= V_{P,2} + U_{i,dc}^{(SDS-4B)}, \quad V_{f,dc}^{(SDS-4B)} = V_{T,2} + U_{f,dc}^{(SDS-4B)} \\ V_{P,k} &= Z_P \left( \frac{1}{R} - \frac{1}{s_k} \right), \quad V_{T,k} = Z_T \left( \frac{1}{R} - \frac{1}{x_k} \right); \quad k = 1, 2 \\ U_{i,dc}^{(SDS-4B)} &= -\nabla_{x_1} \ln(\varphi_i^T(x_1, x_2)) \cdot \nabla_{s_1}, \quad \xi = \frac{Z_T - Z_P}{v} \\ U_{f,dc}^{(SDS-4B)} &= -\nabla_{s_1} \ln(\varphi_f^{p*}(s_1, s_2)) \cdot \nabla_{x_1} \end{aligned} \right\}. \quad (7)$$

Here, for concreteness, electrons  $e_1$  and  $e_2$  are viewed as undergoing double and single scatterings, respectively. The underlying assumption is that the bound-state wave function of  $e_1$  ( $e_2$ ) is distorted (undistorted) by the presence of the Coulomb fields from  $P - e_1(P - e_2)$  in the entrance channel and  $T - e_1(T - e_2)$  in the exit channel. The same transition probability is obtained for the other way around, i.e. when electrons  $e_1$  and  $e_2$  are considered to be captured through single and double scatterings, respectively. This exchange effect is achieved by the permutation operator  $P_{12}$  through the form of the symmetrization operator  $(1 + P_{12})/\sqrt{2}$ .

## 2.2 The CDW-4B method (prior and post) for SC

As seen from these formulae, there is a great resemblance between the SDS-4B method for DC [18] and the CDW-4B method for SC [21]. To make this feature more explicit, we need also the transition amplitudes in the CDW-4B method for SC in the process symbolized as:

$$Z_P + (Z_T; e_1, e_2)_i \longrightarrow (Z_P, e_1)_{f_1} + (Z_T, e_2)_{f_2}, \quad (8)$$

where  $\{f_1, f_2\} \equiv f'$  is the set of the final quantum numbers of the two hydrogenlike atomic systems (there will be no confusion to hereafter relabel  $f'$  as  $f$ , for simplicity). The prior and post transition amplitudes  $T_{if,sc}^{(CDW-4B)\mp}$  in the CDW-4B method [21] for single capture in process (8) are defined by:

$$T_{if,sc}^{(CDW-4B)-}(\eta) = \iiint d\mathbf{x}_1 d\mathbf{x}_2 d\mathbf{R} \mathcal{E}_{sc} \times \varphi_{f_1}^{P*}(\mathbf{s}_1) \varphi_{f_2}^{T*}(\mathbf{x}_2) \frac{1 + P_{12}}{\sqrt{2}} D_{T,\text{eff}}^{-*}(\mathbf{x}_1) V_{i,sc}^{(CDW-4B)} \varphi_i^T(\mathbf{x}_1, \mathbf{x}_2) D_P^+(\mathbf{s}_1), \quad (9)$$

$$T_{if,sc}^{(CDW-4B)+}(\eta) = \iiint ds_1 ds_2 d\mathbf{R} \mathcal{E}_{sc} \times \varphi_i^T(\mathbf{x}_1, \mathbf{x}_2) \frac{1 + P_{12}}{\sqrt{2}} D_P^+(\mathbf{s}_1) V_{f,sc}^{(CDW-4B)} \varphi_{f_1}^{P*}(\mathbf{s}_1) \varphi_{f_2}^{T*}(\mathbf{x}_2) D_{T,\text{eff}}^{-*}(\mathbf{x}_1), \quad (10)$$

$$V_{i,sc}^{(CDW-4B)} = V_{i,dc}^{(SDS-4B)}, \quad (11)$$

$$V_{f,sc}^{(CDW-4B)} = (V_{P,2} + V_{12}) - \nabla_{s_1} \ln(\varphi_{f_2}^{T*}(\mathbf{x}_2) \varphi_{f_1}^{P*}(\mathbf{s}_1)) \cdot \nabla_{x_1}, \quad (12)$$

$$V_{12} = \frac{1}{x_{12}} - \frac{1}{x_1}, \quad (13)$$

$$\left. \begin{aligned} \mathcal{E}_{sc} &= e^{i\alpha_{sc} \cdot s_1 + i\beta_{sc} \cdot x_1} \\ D_{T,\text{eff}}^-(\mathbf{x}_k) &= N^-(v_{T,\text{eff}}) {}_1F_1(-iv_{T,\text{eff}}, 1, -ivx_k - i\mathbf{v} \cdot \mathbf{x}_k); \quad k = 1, 2 \\ N^-(v_{T,\text{eff}}) &= e^{\pi v_{T,\text{eff}}/2} \Gamma(1 + iv_{T,\text{eff}}) \\ v_{T,\text{eff}} &= \frac{Z_{T,\text{eff}}}{v}, \quad Z_{T,\text{eff}} = Z_T - 1 \\ \alpha_{sc} &= \eta - v_{sc}^+ \mathbf{v}, \quad \beta_{sc} = -\eta - v_{sc}^- \mathbf{v}, \quad \alpha_{sc} + \beta_{sc} = -\mathbf{v} \\ v_{sc}^\pm &= \frac{1}{2} \pm \frac{\Delta E_{sc}}{v^2}, \quad \Delta E_{sc} = (E_{f_1}^P + E_{f_2}^T) - E_i^T \end{aligned} \right\}. \quad (14)$$

Here,  $\varphi_{f_k}^K$  and  $E_{f_k}^K$  are the respective final bound-state wave function and the binding energy of the hydrogenlike system  $(Z_K, e_k)_{f_k}$  ( $K=P, T; k = 1, 2$ ). In Eqs. (9) and (10), electron  $e_1$  is captured through a double collision ( $P - e_1 - T$ ) and this leads to formation of  $(Z_P, e_1)_{f_1}$  described by  $\varphi_{f_1}^P(s_1)$ . On the other hand, electron  $e_2$  is bound in the final state  $\varphi_{f_2}^T(\mathbf{x}_2)$  of the target remainder,  $(Z_T, e_2)_{f_2}$ . The transition amplitudes  $T_{if,sc}^{(CDW-4B)\mp}$  for this combination of the collisional events are symmetrized. Here too, the same probability is obtained when electrons  $e_1$  and  $e_2$  exchange their roles. Alternatively, the symmetrization operator  $(1 + P_{12})/\sqrt{2}$  from Eqs. (9) and (10) can be omitted, in which case all the ensuing cross sections (total  $Q_{if}$ , differential  $dQ_{if}/d\Omega$ ) are to be multiplied by 2, as has been done in Ref. [21].

In principle, the electron  $e_2$  can contribute to the probability of capture of electron  $e_1$  in SC from (8). This could be achieved by the velocity-matching single collisions ( $P - e_2$ ) through the Coulomb interaction potential  $V_{p,2} = Z_P(1/R - 1/s_2)$  in Eqs. (9) and (10). Such scattering events can be mediated by the static  $e_1 - e_2$  correlations in the initial state  $\varphi_i^T(\mathbf{x}_1, \mathbf{x}_2)$  of the target  $(Z_T; e_1, e_2)_i$ .

The similarity is obvious between the prior transition amplitudes (5) and (9) in the SDS-4B and CDW-4B methods for DC and SC in processes (1) and (8), respectively. This occurs because the two methods describe the entrance channel in the same way for DC in (1) and SC in (8). However, processes (1) for DC and (8) for SC differ in their exit channels and so do the corresponding descriptions by the SDS-4B and CDW-4B methods, respectively.

This latter dissimilarity is most transparent in the post transition amplitudes (6) for DC and (10) for SC, especially regarding the perturbation potentials. Compared to Eq. (6) for DC, there is an extra short-range interaction  $V_{12} = 1/x_{12} - 1/x_1$  in the perturbation from Eq. (13) for SC. A partial account of the electron-electron dynamic correlations for SC is achieved by using  $1/x_{12}$  in the full perturbation interaction from Eq. (13). For DC, potential  $1/x_{12}$  is absent from the perturbation in Eq. (6) since it is absorbed in the bound-state eigenvalue problem for the heliumlike system  $(Z_P; e_1, e_2)_f$  in the exit channel of DC in (1).

Another difference exists between Eqs. (6) and (10) and that is in the electronic part of the distortions of the final unperturbed states. In both Eqs. (6) and (10), the related common distorting factor is the one-electron Coulomb continuum wave functions in the exit channels. However, this function is placed on two different nuclear charges, i.e. the target bare nuclear charge  $Z_T$  for DC in (1) and the point charge  $Z_{T,\text{eff}} = Z_T - 1$  of the target remainder  $(Z_T, e_2)_{f_2}$  for SC in (8). Here,  $Z_T - 1$  is the screened target nuclear charge (the target bare nuclear charge  $Z_T$  reduced by the unit charge of electron  $e_2$ ).

By definition, the final bound-state wave functions are different for SC and DC. Thus, the final bound-state heliumlike wave function  $\varphi_f^P(s_1, s_2)$  is for the nuclear charge  $Z_P$  of P in DC from (1). In SC from (8), the two final bound-state hydrogenlike wave functions are on two different nuclear charges, i.e.  $\varphi_{f_1}^P(s_1)$  is for  $Z_P$ , whereas  $\varphi_{f_2}^T(\mathbf{x}_2)$  is for  $Z_T - 1$ .

Moreover, DC and SC collisions differ in the critically important electron translation factors. Two and one such factors associated with transfer of two and one electrons are present in  $\mathcal{E}_{dc}$  and  $\mathcal{E}_{sc}$  from Eqs. (3) and (14), respectively. As discussed, electron

$e_2$  stays with the target remainder  $(Z_T, e_2)_f$  in the exit channel of SC in process (8). Therefore, the translation factor for electron  $e_2$  is absent from the exponential  $\mathcal{E}_{sc}$  in Eq. (14).

The advantage of juxtaposing the transition amplitudes for (1) and (8) is that  $T_{if,dc}^{(SDS-4B)\mp}$  for DC and  $T_{if,sc}^{(CDW-4B)\mp}$  for SC can be deduced from each other. Thus,  $T_{if,sc}^{(CDW-4B)-}$  would follow if in  $T_{if,dc}^{(SDS-4B)-}$  these changes are made:  $\varphi_f^p(s_1, s_2) \rightarrow \varphi_{f_1}^p(s_1)\varphi_{f_2}^T(s_2)$ ,  $v_T = Z_T/v \rightarrow v_{T,eff} = Z_{T,eff}/v$ ,  $\mathcal{E}_{dc} \rightarrow \mathcal{E}_{sc}$ ,  $\alpha_{dc} \rightarrow \alpha_{sc}$ ,  $\beta_{dc} \rightarrow \beta_{sc}$  and  $v_{dc}^\pm \rightarrow v_{sc}^\pm$ . Conversely,  $T_{if,dc}^{(SDS-4B)-}$  would emerge if in  $T_{if,sc}^{(CDW-4B)-}$  we redefine:  $\varphi_{f_1}^p(s_1)\varphi_{f_2}^T(s_2) \rightarrow \varphi_f^p(s_1, s_2)$ ,  $v_{T,eff} = Z_{T,eff}/v \rightarrow v_T = Z_T/v$ ,  $\mathcal{E}_{sc} \rightarrow \mathcal{E}_{dc}$ ,  $\alpha_{sc} \rightarrow \alpha_{dc}$ ,  $\beta_{sc} \rightarrow \beta_{dc}$  and  $v_{sc}^\pm \rightarrow v_{dc}^\pm$ . These redefinitions, supplemented by the alterations: (a)  $V_{T,k} \rightarrow V_{P,k} + V_{12}$  in  $V_{f,dc}^{(SDS-4B)}$  from  $T_{if,dc}^{(SDS-4B)+}$  would yield  $T_{if,sc}^{(CDW-4B)+}$  and (b)  $V_{P,k} + V_{12} \rightarrow V_{T,k}$  in  $V_{f,sc}^{(CDW-4B)}$  from  $T_{if,sc}^{(CDW-4B)+}$  would give  $T_{if,dc}^{(SDS-4B)+}$ .

### 2.3 The CB1-4B method (prior and post) for DC

$$T_{if,dc}^{(CB1-4B)-}(\eta) = \iiint dx_1 dx_2 dR \mathcal{E}_{dc} (vR - v \cdot R)^{2i\xi} \times \varphi_f^{p*}(s_1, s_2) V_{i,dc}^{(CB1-4B)} \varphi_i^T(x_1, x_2), \quad (15)$$

$$T_{if,dc}^{(CB1-4B)+}(\eta) = \iiint ds_1 ds_2 dR \mathcal{E}_{dc} (vR + v \cdot R)^{-2i\xi} \times \varphi_f^{p*}(s_1, s_2) V_{f,dc}^{(CB1-4B)} \varphi_i^T(x_1, x_2), \quad (16)$$

$$V_{i,dc}^{(CB1-4B)} = V_{P,1} + V_{P,2}, \quad V_{f,dc}^{(CB1-4B)} = V_{T,1} + V_{T,2}. \quad (17)$$

### 2.4 The CDW-4B method (prior and post) for DC

$$T_{if,dc}^{(CDW-4B)-}(\eta) = \iiint dx_1 dx_2 dR \mathcal{E}_{dc} D_T^{-*}(x_1, x_2) \times \varphi_f^{p*}(s_1, s_2) (1 + P_{12}) D_P^+(s_2) V_{i,dc}^{(CDW-4B)} \varphi_i^T(x_1, x_2) D_P^+(s_1), \quad (18)$$

$$T_{if,dc}^{(CDW-4B)+}(\eta) = \iiint ds_1 ds_2 dR \mathcal{E}_{dc} D_P^+(s_1, s_2) \times \varphi_i^T(x_1, x_2) (1 + P_{12}) D_T^{-*}(x_2) V_{f,dc}^{(CDW-4B)} \varphi_f^{p*}(s_1, s_2) D_T^{-*}(x_1), \quad (19)$$

$$V_{i,dc}^{(CDW-4B)} = U_{i,dc}^{(SDS-4B)}, \quad V_{f,dc}^{(CDW-4B)} = U_{f,dc}^{(SDS-4B)}. \quad (20)$$



## 2.5 The CDW-EIS-4B method (post) for DC

$$T_{if,dc}^{(CDW-EIS-4B)+}(\eta) = \iiint ds_1 ds_2 d\mathbf{R} \mathcal{E}_{dc} D_{P,eik}^+(s_1, s_2) \\ \times \varphi_i^T(\mathbf{x}_1, \mathbf{x}_2)(1 + P_{12})D_T^{-*}(\mathbf{x}_2)V_{f,dc}^{(CDW-EIS-4B)}\varphi_f^{P*}(s_1, s_2)D_T^{-*}(\mathbf{x}_1), \quad (21)$$

$$V_{f,dc}^{(CDW-EIS-4B)} = V_{f,dc}^{(CDW-4B)}. \quad (22)$$

## 2.6 The BCIS-4B method (prior and post) for DC

$$T_{if,dc}^{(BCIS-4B)-}(\eta) = \iiint dx_1 dx_2 d\mathbf{R} \mathcal{E}_{dc} (vR - \mathbf{v} \cdot \mathbf{R})^{-2i\nu_P} \\ \times \varphi_f^{P*}(s_1, s_2)V_{i,dc}^{(BCIS-4B)}\varphi_i^T(\mathbf{x}_1, \mathbf{x}_2)D_T^{-*}(\mathbf{x}_1, \mathbf{x}_2), \quad (23)$$

$$T_{if,dc}^{(BCIS-4B)+}(\eta) = \iiint ds_1 ds_2 d\mathbf{R} \mathcal{E}_{dc} (vR + \mathbf{v} \cdot \mathbf{R})^{-2i\nu_T} \\ \times \varphi_f^{P*}(s_1, s_2)V_{f,dc}^{(BCIS-4B)}\varphi_i^T(\mathbf{x}_1, \mathbf{x}_2)D_P^+(s_1, s_2). \quad (24)$$

$$V_{i,dc}^{(BCIS-4B)} = V_{i,dc}^{(CB1-4B)}, \quad V_{f,dc}^{(BCIS-4B)} = V_{f,dc}^{(CB1-4B)}. \quad (25)$$

## 2.7 The BDW-4B method (prior and post) for DC

$$T_{if,dc}^{(BDW-4B)-}(\eta) = \iiint dx_1 dx_2 d\mathbf{R} \mathcal{E}_{dc} (vR + \mathbf{v} \cdot \mathbf{R})^{-2i\nu_T} \\ \times \varphi_f^{P*}(s_1, s_2)(1 + P_{12})D_P^+(s_2)V_{i,dc}^{(BDW-4B)}\varphi_i^T(\mathbf{x}_1, \mathbf{x}_2)D_T^+(s_1), \quad (26)$$

$$T_{if,dc}^{(BDW-4B)+}(\eta) = \iiint ds_1 ds_2 d\mathbf{R} \mathcal{E}_{dc} (vR - \mathbf{v} \cdot \mathbf{R})^{-2i\nu_P} \\ \times \varphi_i^T(\mathbf{x}_1, \mathbf{x}_2)(1 + P_{12})D_T^{-*}(\mathbf{x}_2)V_{f,dc}^{(BDW-4B)}\varphi_f^{P*}(s_1, s_2)D_T^{-*}(\mathbf{x}_1), \quad (27)$$

$$V_{i,dc}^{(BDW-4B)} = V_{i,dc}^{(CDW-4B)}, \quad V_{f,dc}^{(BDW-4B)} = V_{f,dc}^{(CDW-4B)}. \quad (28)$$

## 2.8 Total cross sections

The total cross sections  $Q_{if}^{\mp}$  for SC and DC are computed from the usual formulae:

$$Q_{if}^{\mp}(a_0^2) = \int d\eta \left| \frac{T_{if}^{\mp}(\eta)}{2\pi v} \right|^2, \quad (29)$$

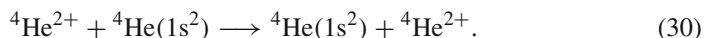
where  $a_0$  is the Bohr radius. In all the illustrations (figures), these cross sections are expressed in units of  $\text{cm}^2$  using the constant  $\pi a_0^2 \approx 8.797 \times 10^{-17} \text{cm}^2$ . Generally, depending on the values of the magnetic quantum numbers  $m_i$  and  $m_f$  of the initial and final states, respectively, the integrands  $T_{if}^{\mp}(\eta)$  in (29) may explicitly depend on angle  $\phi_\eta \in [0, 2\pi]$  of  $\eta$ . However, a trivial analytical integration over  $\phi_\eta$  in (29) always gives  $2\pi$ . For the presently considered initial and final ground states,  $T_{if}^{\mp}(\eta)$  is independent on  $\phi_\eta$  and the integral over this angle yields  $2\pi$ .

We computed  $Q_{if}^{\mp}$  by carrying out the multiple numerical quadratures (3-dimensional in the CB1-4B method, 4-dimensional in the CDW-4B and 5-dimensional in the BCIS-4B, BDW-4B and SDS-4B methods). The results from the CDW-EIS-4B method (4-dimensional quadratures) are taken from Refs. [16, 17]. We use the Gauss-Legendre quadrature rule in the CB1-4B, CDW-4B, BCIS-4B, BDW-4B and SDS-4B methods. In these methods, presently applied to the symmetric case  $Z_T = Z_P = 2$  of process (1), i.e.  ${}^4\text{He}^{2+} + {}^4\text{He}(1s^2) \rightarrow {}^4\text{He}(1s^2) + {}^4\text{He}^{2+}$ , the explicit computations confirmed that there is no post-prior discrepancy, as expected.

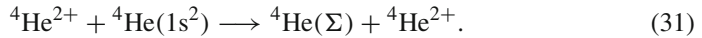
Regarding differential cross sections  $dQ_{if}^{\mp}/d\Omega$ , the CDW-4B and CDW-EIS-4B methods always use the highly oscillatory Fourier-Bessel numerical integration for both the homo-nuclear ( $Z_P = Z_T$ ) and hetero-nuclear ( $Z_P \neq Z_T$ ) charges. However, for some special cases, this integration is avoided in the CB1-4B, BCIS-4B, BDW-4B and SDS-4B methods for which the angular distributions  $dQ_{if}^{\mp}/d\Omega$  are obtained by squaring the absolute values of the already available transition amplitudes  $T_{if}^{\mp}(\eta)$ . This is the case in the post and prior forms of the CB1-4B method for either  $Z_P = 2$  or  $Z_T = 2$ . The same advantage is also encountered in the BCIS-4B method (prior:  $Z_P = 2$ , post:  $Z_T = 2$ ), the BDW-4B method (prior:  $Z_T = 2$ , post:  $Z_P = 2$ ) as well as in the prior and post forms of the SDS-4B method for either  $Z_P = 1$  or  $Z_T = 1$ .

## 3 Results and discussion

The cross sections  $Q$  with the heavy mass limit ( $1/M_{P,T} \ll 1$ ) in the CB1-4B, CDW-4B, CDW-EIS-4B, BCIS-4B, BDW-4B and SDS-4B methods are illustrated in five figures. For DC in the  $\alpha - \text{He}$  collisions, the results from these six methods to be analyzed concern only the ground-to-ground state transition. They are all obtained with the one-parameter Hylleraas [22] wave function of helium in the entrance and exit channels. The collisions of this type are written as:



The only experimental data on  $Q$  for this process are from Refs. [23] and [24]. All the other measured cross sections  $Q$  on DC to be shown are from Refs. [25–37] and they refer to the state-summed transitions ( $1s^2 \rightarrow \Sigma$ ), i.e. for a process with all final bound states (ground and excited) of helium:



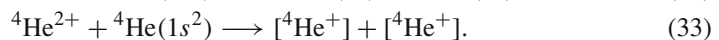
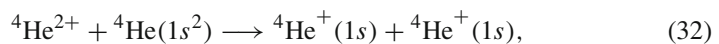
Using the cold target recoil ion momentum spectroscopy (COLTRIMS), Refs. [24, 38] reported the experimentally measured cross sections  $dQ/d\Omega$  for both the ground and excited final states in the  $\text{He}^{2+} + \text{He}(1s^2) \rightarrow \text{He}(\text{ground, excited}) + \text{He}^{2+}$  collisions. Therein, excited-state differential cross sections have been found to be small relative to their counterparts for the ground-to-ground state transitions. The same applies to total cross sections when integrating  $dQ/d\Omega$  over the solid angle  $\Omega$ .

Thus, it is still meaningful to compare the theoretical cross sections  $Q$  for (30) with the experimental data for (31). We shall do that with no scaling of  $Q$  for (30), i.e. without any approximate inclusion of the final excited states of helium in (31). The smallness of the measured excited-state contributions to DC in the  $\alpha + \text{He}(i) \rightarrow \text{He}(f) + \alpha$  collisions is due to the dominance of the resonant transition  $\text{He}(1s^2) \rightarrow \text{He}(1s^2)$  which is process (30).

In Figs. 1–5, several important aspects of DC are addressed using the mentioned six quantum-mechanical four-body perturbative methods with correct boundary conditions. Such aspects include the assessment of the relative performance of these theories with respect to all the existing experimental data from different measurements at 100–6000 keV. Also evaluated are the competing mechanisms for DC described by these different DW methods.

Moreover, assessed are the contributions due to the two parts of the complete distorting potentials, the electrostatic pairwise Coulomb interactions (electron-nucleus) and the cross-kinetic energy operator potentials. Further, when it comes to the reliability of representing theoretically the measurements, special attention is paid to differentiate between the one- and two-channel electronic distortions. To put the analysis in context and perspective, the results for DC are juxtaposed to those for SC. The aim is to check how the past successful experience of the DW theories with correct boundary conditions for SC would translate to DC.

Thus, the first insight into the relative strength of DC can be gained by visualizing its cross sections alongside the corresponding results for SC in the same  $\alpha - \text{He}$  collisional system with the two exit channels according to:



Here, symbol  $[{}^4\text{He}^+]$  denotes that the  ${}^4\text{He}^+$  ion is any state. Regarding theories for (32), only the values of  $Q$  in the CB1–4B and CDW–4B methods will be used. For both methods, we will employ the ground-state helium wave functions of Hylleraas [22] and Silverman *et al.* [39]. As is customary, these predictions for  $Q$  will be multiplied

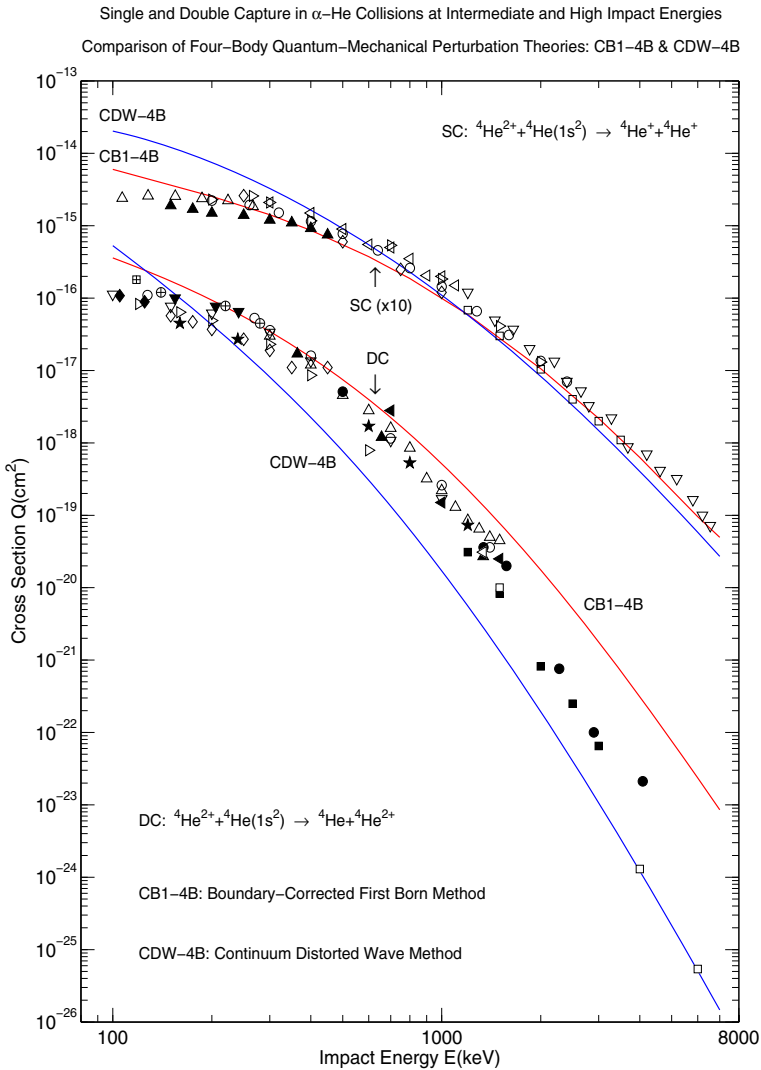


**Fig. 1** Total cross sections  $Q$  ( $\text{cm}^2$ ) versus impact energy  $E$  (keV) for single capture, SC (top), and double capture, DC (bottom), in the  $\alpha$  – He collisions. Theories (the prior form) are for the initial and final ground states. This is the case only in two measurements on DC: Zastrow *et al.* [23] (JET) and Schöffler *et al.* [24] (COLTRIMS). All the remaining measured cross sections on SC and DC are for capture into any final bound state. For the ground-state helium wave functions, the theories employ the correlated closed-shell orbitals ( $1s1s'$ ) of Silverman *et al.* [39] for SC in the entrance channel and the uncorrelated open-shell orbitals ( $1s1s$ ) of Hylleraas [22] for DC in the entrance as well as exit channels. Experimental data: SC (top)  $\blacktriangle$  [25],  $\triangleleft$  [26],  $\nabla$  [40],  $\circ$  [41],  $\triangleright$  [42],  $\square$  [27],  $\Delta$  [43],  $\triangle$  [44]. DC (bottom):  $\diamond$  [25],  $\Delta$  [26],  $\nabla$  [42],  $\blacksquare$  [27],  $\blacktriangle$  [28],  $\nabla$  [29],  $\blacklozenge$  [30],  $\circ$  [31],  $\blacktriangleleft$  [32],  $\triangleleft$  [33],  $\triangleright$  [34],  $\oplus$  [35],  $\square$  [36],  $\bullet$  [37],  $\boxplus$  [23],  $\star$  [24]. For details, see the main text (color online)

by 1.202 (the Oppenheimer scaling factor) to connect them (albeit approximately) with process (33) for which the experimental data are available [25–27, 40–44].

It is clear that DC is weaker than SC since the former is a higher-order process (more involved), which then necessarily has a smaller chance for occurring. Even if capture of each electron is completely independent, as in the IPM, the product probability for DC is smaller than the individual probabilities for each SC. This is valid for physical probabilities that must always be smaller than or equal to unity (the probability conservation law).

In the CDW-4B method, there is yet another reason for cross sections  $Q$  to be smaller in DC than in SC. It is the occurrence of the stronger oscillations (yielding more intense destructive interference effects) from four than from two electronic Kummer functions in DC and SC, respectively. These oscillations are not damped by the cross-kinetic energy parts of the perturbation potentials at fixed electronic distances (from the nuclei) in the bound-states. However, at decreasing heavy particle separations  $R$  (for fixed electronic distances in the bound-states), such oscillations can be mitigated by the Coulomb potentials of the type  $\sim 1/R$  that are present in the electrostatic perturbation potentials from the CDW-4B method for SC. Potentials  $\sim 1/R$  are absent from the perturbation interactions in the CDW-4B and BDW-4B methods for DC (but present in the BCIS-4B and SDS-4B methods for DC).

The results for SC and DC are illustrated in Fig. 1 at 80–8000 keV by using the CB1-4B and CDW-4B methods together with the measurements. The top and the bottom sets of the displayed data are for SC and DC, respectively. For clarity, all the results for SC are multiplied by 10. The disparity between the SC and DC data is seen to vary strongly with changes in the impact energy  $E$  in both theoretical and experimental sets. For example, in the CDW-4B method, we have  $Q_{sc}^{(CDW-4B)}/Q_{dc}^{(CDW-4B)} \approx 4$  and  $Q_{sc}^{(CDW-4B)}/Q_{dc}^{(CDW-4B)} \approx 230000$  at 100 and 8000 keV, respectively. In other words, the lines of cross sections for DC in the CDW-4B method decline far much faster than those for SC. The same or a similar conclusion can also be drawn with the CB1-4B method as well as with the measured cross sections.

Another striking observation can be made in Fig. 1 when comparing the CB1-4B and CDW-4B methods for one process at a time (SC or DC). Thus, at e.g. 8000 keV, we have  $Q_{sc}^{(CB1-4B)}/Q_{sc}^{(CDW-4B)} \approx 1.7$  for SC and  $Q_{dc}^{(CB1-4B)}/Q_{dc}^{(CDW-4B)} \approx 70$  for DC. Moreover, the widely different intersection energies,  $\sim 1500$  and  $\sim 120$  keV, are seen for the line pairs for SC (top) and DC (bottom), respectively.

For SC, below and above 1500 keV, the CB1-4B method underestimates and overestimates the CDW-4B method, respectively. Such underestimations and overestimations are relatively mild. This indicates that at 80–8000 keV, an inclusion of the intermediate ionizing continua in the entrance and exit channels for SC in the CDW-4B method (one electronic full Coulomb wave per channel) is not overly influential on either the magnitude or the line-shapes of the computed  $Q$  relative to the CB1-4B method. This latter method completely ignores the said second-order effects (the intermediate ionization of either electron). Most importantly, it is noted that the CB1-4B (at  $E > 100$  keV) and CDW-4B (at  $E > 200$  keV) methods for SC exhibit a very good or excellent performance when compared to the experimental data.

In Fig. 1, the experimental data from different measurements, juxtaposed for SC and DC, also merit an appropriate comment. All the measured cross sections for SC from various recordings are in mutual accord and lined up next to each other without some inordinate dispersions. This offers a reliable basis for robust tests of adequacy of different theories. An opposite situation is encountered in DC, where cross sections from various measurements differ by sizable factors of 3, 4, 6 and even 20 at  $E = 200, 600, 1500$  and  $4000$  keV, respectively. Such an increasing discrepancy with rising energy  $E$  is most pronounced above 3 MeV where only three controversial experimental data points are available from two different measurements [36, 37].

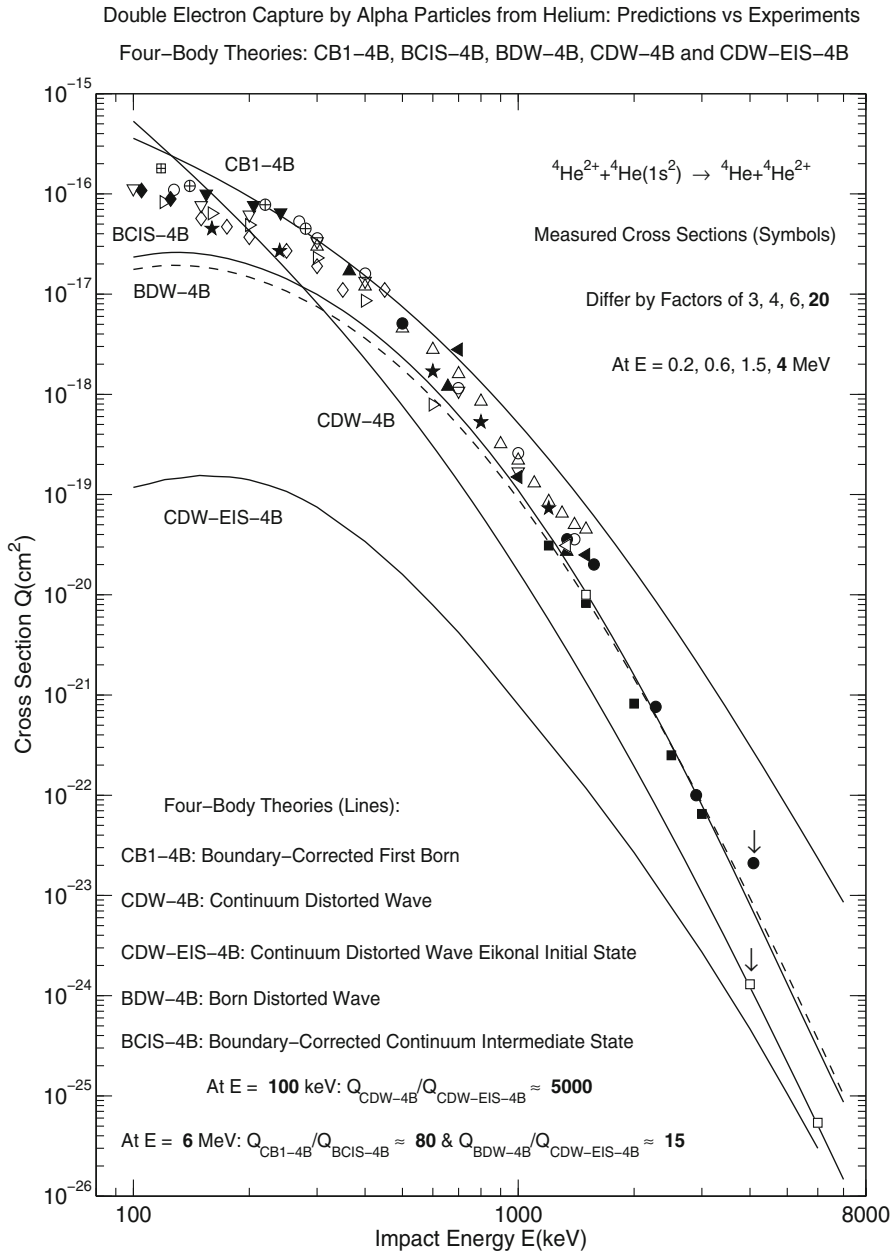
In particular, at  $4000$  [36] and  $4080$  keV [37], the measured cross sections differ by an enormous factor of about 20. This situation underscores the need for some new, more precise measurements on  $Q$  at higher energies, e.g. by COLTRIMS [24, 38, 45]. Reduced accuracy of the measured cross sections for DC compared to SC is partially caused by the weakness of the former process. Another possible reason could be in considerable difficulty to experimentally distinguish between capture of both electrons involving the same collision  $\text{He}^{2+} - \text{He}$  from sequential DC encompassing two SC collisions with different targets, He and the rest gas G ( $\text{He}^{2+} + \text{He} \rightarrow \text{He}^+ + \text{He}^+$  followed by  $\text{He}^+ + G \rightarrow \text{He} + G^+$ ).

Figure 2 compares the CB1-4B, CDW-4B, CDW-EIS-4B, BCIS-4B and BDW-4B methods with the measurements. Herein, the status of different DW theories is self-evident in plain view. Specifically, there is an extreme model-dependence of DC manifested in the orders of magnitude discrepancy even when only the second-order theories are considered. For instance, a factor of 5000 discrepancy is seen between the CDW-4B and CDW-EIS-4B methods at  $100$  keV. Any shortcomings of the theory, yielding no severe consequences for SC, could be exacerbated for DC.

This enhanced sensitivity of the theory is due to the discussed smallness of the cross sections for DC relative to SC. Thus, approximating e.g. the electronic full Coulomb waves from the CDW-4B method by their eikonal phases in the CDW-EIS-4B method for SC appears to be largely innocuous at moderately high energies. For SC, according to e.g. Ref. [3], when  $E$  decreases, such a replacement becomes even beneficial regarding the experimental data because around the Massey peaks for  $Q$  the CDW-EIS-4B method outperforms the CDW-4B method.

However, in DC (Fig. 2), precisely around the Massey peak (i.e. around  $100$  keV), exactly the same eikonal approximation in the CDW-EIS-4B method underestimates the experimental data by about three orders of magnitude. Even at  $3000$  keV, the CDW-EIS-4B method underestimates the measured  $Q$  by a factor of 30. This complete breakdown of the CDW-EIS-4B method for DC within the usual validity domain of this theory is caused by the 'multiplication effect' in the eikonal electronic distortions. This effect refers to the appearance of the product of the two eikonal phases (one for each captured electron) in DC compared with only one such eikonal phase in SC. Each electronic eikonal phase in the CDW-EIS-4B method carries an error and, therefore, multiplication of two such phases in DC is bound to worsen the accuracy of the predictions by this theory.

Nevertheless, it is surprising that this inadequacy of the CDW-EIS-4B method for DC is so pronounced. In retrospect then, the marked inappropriateness of the electronic eikonalization of the full Coulomb waves in DC could question anew the success of the



**Fig. 2** Total cross sections  $Q(\text{cm}^2)$  versus impact energy  $E(\text{keV})$  for double capture, DC, in the  $\alpha - \text{He}$  collisions. Theories are for the initial and final ground states of helium. This is the case only in two measurements: Zastrow *et al.* [23] (JET) and Schöffler *et al.* [24] (COLTRIMS). All the remaining measured cross sections are for capture into any final helium bound state. For the ground-state helium wave functions, the theories employ the uncorrelated open-shell orbitals ( $1s1s$ ) of Hylleraas [22] in the entrance and exit channels. The CB1-4B, CDW-4B, BCIS-4B and BDW-4B methods are in the prior forms, whereas the CDW-EIS-4B method is in the post form. Experimental data:  $\diamond$  [25],  $\triangle$  [26],  $\nabla$  [42],  $\blacksquare$  [27],  $\blacktriangle$  [28],  $\blacktriangledown$  [29],  $\blacklozenge$  [30],  $\circ$  [31],  $\blacktriangleleft$  [32],  $\blacktriangleleft$  [33],  $\triangleright$  [34],  $\oplus$  [35],  $\square$  [36],  $\bullet$  [37],  $\boxplus$  [23],  $\star$  [24]. For details, see the main text

CDW-EIS-4B method for SC. In fact, there is no physical reason for which a further approximation to the CDW-4B method [11] (as the one in the CDW-EIS-4B method [16, 17]) should bring any advantage. In the past computations on  $Q$  for SC, one of the main motivations for using the CDW-EIS-4B method was in its better description of merely the Massey peak area than in the CDW-4B method. However, at energies above those around the Massey peak, the CDW-EIS-4B and CDW-4B methods give very similar results for  $Q$  in SC.

Since the CDW-EIS-4B method [16, 17] approximates the CDW-4B method [11], any difference in the cross sections from these two formalisms should, strictly speaking, be interpreted as a measure of the errors introduced by the former theory, irrespective of the outcome of comparisons with the pertinent experiments. For SC, the discrepancy between the CDW-4B and CDW-EIS-4B methods (especially around the Massey peak) went in a good direction for the latter theory, which was favored by the measurements [3]. In contradistinction, for DC, everything went in a wrong direction for the CDW-EIS-4B method (Fig. 2), as it showed a disastrous performance relative to the experiments [16, 17].

Within the second-order DW theories for single ionization (SI), the eikonal initial state approximation of the electronic full Coulomb wave function in the three-body continuum distorted wave (CDW-3B) method [46] appeared in Ref. [47]. The resulting approximation to the CDW-3B method was the CDW-EIS-3B method. Its extension, the CDW-EIS-4B (equivalently called the modified Coulomb-Born, MCB-4B [48, 49]) method for SI in the  $H^+ - H^-$  collisions (i.e. single electron detachment) gave the best agreement with the experimental data [50] at all energies, ranging from the reaction threshold to the Bethe limit. The CDW-EIS-3B method has been adapted to SC in Ref. [51].

In Ref. [47], the goal of this electronic eikonalization was to counter the lack of normalization of the total scattering wave function in the entrance channel of the CDW-3B method [46] at finite times  $t$  (or at finite  $R$ ). However, it is precisely the electronic eikonalization that is the principal source of the most severe setback in the CDW-EIS-4B method for DC. Thus, resorting to eikonalization to mitigate the alleged impact of normalization on charge exchange is hardly a panacea for a curve bending around the Massey peak, since it works for SC, but fails flagrantly for DC.

As to the status of the other three theories in Fig. 2, the CB1-4B method is favorable relative to the measurements below 900 keV, but considerably overestimates the experimental data above 1000 keV. On the other hand, the CDW-4B method is reasonable, first in a minimal window 100–250 keV, then it becomes quite poor at 300–3500 keV and finally it is excellent at the two farthest experimental data points (4000, 6000 keV) from one measurement [36]. The results of the BCIS-4B and BDW-4B methods are close to each other, but below about 550 keV, they are lower than the measured cross sections. Between 550 and 4000 keV, these latter two methods excellently reproduce the experimental data. Regarding the two contradictory data points at 4000 keV [36] and 4080 keV [37], the lines from the BCIS-4B and BDW-4B methods are closer to the measured cross section from Ref. [37].

The BCIS-4B and BDW-4B method for DC have their Coulomb logarithmic  $R$ -dependent phase factors that oscillate heavily with decreasing  $R$ . In these oscillations in the integrands of the transition amplitudes there are always some destructive



interferences that could diminish the values of  $Q$ . For decreasing  $R$  at fixed electronic distances from the nuclei in the bound-states, such oscillations can be partially reduced by the rising contributions from potential  $Z_p/R$ , if present in the perturbation interactions of the transition amplitudes. Potential  $Z_p/R$  appears in the prior and post forms of the BCIS-4B method, but not in the BDW-4B method.

Because the BDW-4B method does not reduce the destructive interferences in the mentioned oscillations, the line for  $Q$  from this theory should lie beneath its counterpart from the BCIS-4B method. This is indeed the case in Fig. 2 below about 2000 keV, although the discrepancy between the BCIS-4B and BDW-4B methods is relatively mild at all the displayed energies, 100–8000 keV. In any case, even a single Coulomb logarithmic  $R$ -dependent phase factor for DC in the BCIS-4B and BDW-4B methods reduces too much the total cross sections that are, in turn, seen to significantly underestimate the experimental data below about 550 keV.

Taken together, while attempting to reproduce the measured cross sections, none of the five theories in Fig. 2 is fully successful at 100–8000 keV, counting both the magnitude and the line-shapes. At most energies, the BCIS-4B method provides the closest representation of the experimental data. Still, this is incomplete as there is room for improvements to cover more quantitatively energies below 550 keV.

Regarding DC in Figs. 1 and 2, the CB1-4B, CDW-4B, CDW-EIS-4B, BCIS-4B and BDW-4B methods are all based on the same assumption that both electrons are simultaneously transferred by single and/or double collisions in one or two channels. As per Fig. 2, the status of these DW perturbative theories for DC exposed the existing lacunae that should also be the opportunities for further explorations of some alternative descriptions. One of such avenues is the SDS-4B method [18], which offers a complementary mechanism for DC by hybridizing the single and double scatterings in each channel. The outcomes of this approach to DC are illustrated in Figs. 3–5.

We already emphasized that the explicit combination of single and double scatterings per channel in the SDS-4B method for DC is similar to that in the CDW-4B method for SC [21]. Therefore, it is intriguing to find out how such a parallelism between these methods for two different collisions would be reflected in the computed cross sections  $Q$ . To that end, the results in the SDS-4B method for DC and their counterparts in the CDW-4B method for SC are displayed alongside each other in Figs. 3 and 4.

In Fig. 3, shown are the two pairs of the results, one in the CDW-4B method for SC (top) and the other in the SDS-4B method for DC (bottom). Each pair shows the lines with and without perturbation  $V_{p,2} = Z_p(1/R - 1/s_2)$  in the composite residual interaction  $V_{i,dc}^{(SDS-4B)} = V_{i,sc}^{(CDW-4B)} = V_{p,2} - \nabla_{x_1} \ln(\varphi_i^T) \cdot \nabla_{s_1}$ .

It is seen in Fig. 3 that the pairs of the lines from SC and DC are quite alike. The lines in SC intersect each other at about 1200 keV and similarly for DC at about 1750 keV. Below these crossing energies, the lines without  $V_{p,2}$  are lower than those with  $V_{p,2}$ , while above 1200 for SC and above 1750 keV for DC the situation is just the reverse. For the neglected  $V_{p,2}$ , the ensuing weaker complete perturbation reduces the capture probability with decreasing  $E$  and, thus, yields smaller cross sections  $Q$ . Such a reduction is by about a factor of 2 stronger in DC than in SC. Here, a general feature is observed [52] (p. 289), according to which the same type of errors in  $Q$  (systematic,

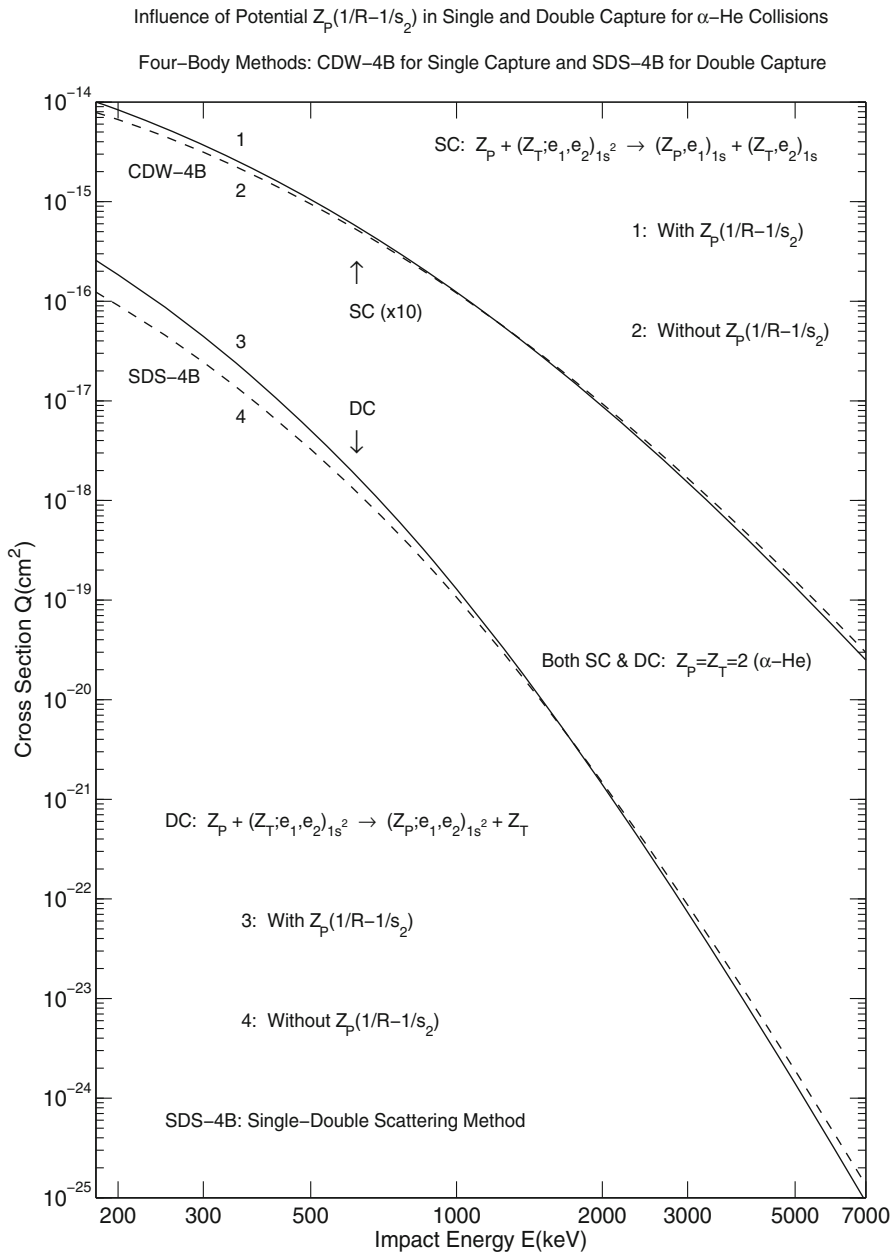


**Fig. 3** Total cross sections  $Q(\text{cm}^2)$  versus impact energy  $E(\text{keV})$  for single capture, SC (top), and double capture, DC (bottom), in the  $\alpha - \text{He}$  collisions. Theories (the prior form) are for the uncorrelated open-shell ground-state orbitals ( $1s\ 1s$ ) of Hylleraas [22] in SC (entrance channel) and DC (entrance and exit channels). Computations performed with and without potential  $V_{p,2} = 2(1/R - 1/s_2)$  from the complete interaction in the perturbation potential operator:  $V_{p,2} - \nabla_{x_1} \ln \varphi_i^T \cdot \nabla_{s_1}$ . In SC, potential  $V_{p,2}$  describes indirect capture of active electron  $e_1$  by way of the interaction between the projectile nucleus P with the non-transferred electron  $e_2$ . For details, see the main text

statistical in theories and experiments alike) made in SC and DC can be at least twice larger for double than for single capture collisional events.

At higher energies in Fig. 3, the complete perturbation tends to give smaller  $Q$  relative to the case when  $V_{p,2}$  is ignored. The implication is that with increasing  $E$ , there is an enhanced destructive interference between the one-center ( $V_{p,2}$ ) and two-center ( $\nabla_{x_1} \ln(\varphi_i^T) \cdot \nabla_{s_1}$ ) contributions coming from the complete perturbation interaction  $V_{p,2} - \nabla_{x_1} \ln(\varphi_i^T) \cdot \nabla_{s_1}$ .

This is expected since with the augmented  $E$ , double scatterings (two-center effects of the Thomas type) become more important than single scatterings (one-center effects of kinematic capture). Insightful as it might be, Fig. 3 is still mostly qualitative as it focuses primarily on the line-shape patterns of  $Q$  versus  $E$  for SC and DC. Yet, even with the restricted focus, there is nevertheless a quantitative hint from Fig. 3. Namely, a line-shape, being an energy dependence of a total cross section, can inform about the rate of decline of  $Q(E)$  with rising  $E$ .

It is this rate in Fig. 3 that is much faster in DC with the SDS-4B method than in SC with the CDW-4B method. Such a finding coheres with the like observation in Fig. 2 for DC and SC from the CDW-4B method alone. The results for  $Q$  from the CDW-4B method are intentionally not included in Fig. 3, as this figure is devoted solely to the dependence of the line-shapes on  $V_{p,2}$ . By definition, potential  $V_{p,2}$  is absent from the perturbation interaction  $V_{i,dc}^{(CDW-4B)}$  for DC in the CDW-4B method.

To go beyond the qualitative aspect (the line-shapes), Fig. 4 gives the relevant full quantitative information on  $Q$  obtained with the complete perturbation interactions in the prior forms of the SDS-4B method for DC (bottom) as well as the CDW-4B method for SC (top) and DC (bottom). Specifically for DC at 200–8000 keV, Fig. 4 shows that the CDW-4B method considerably underestimates the SDS-4B method. Importantly, however, it is the SDS-4B method for DC that is seen here to successively reproduce most of the experimental data. Moreover, by reference to the top part of Fig. 4, it follows that the same single-double scattering mechanism per channel is capable of securing a comparable adequacy (with respect to the measurements) at similar energies  $E$  for SC and DC in the CDW-4B and SDS-4B methods, respectively.

Such a finding shows that the lowest-order of the Dodd-Greider perturbation series expansion [1] for DC can be as successful as its counterpart for SC. For this to happen, however, it is less likely that DC in the  $\alpha - \text{He}$  collisions should proceed with simultaneous capture of both electrons by double Thomas-type scatterings in two channels as prescribed by the CDW-4B method. Instead, DC appears to be more probable if, in both channels, one electron undergoes double collisions, while the other electron is transferred by single collisions, as envisaged by the SDS-4B method.

In the CDW-4B method for DC, two paths with simultaneous double collisions for each electron per channel are too demanding and, thus, less likely. This pathway requires a highly coordinated motion of both electrons to bring them to almost the same spatial location at nearly the same time, so that they could be both captured via the identical Thomas-type two-step collisions. Such a strict requirement for DC is obviated in the SDS-4B method. While combining the one- and two-step mechanisms, the SDS-4B method creates more possibilities for two electrons and two nuclei.

The enhanced freedom increases their chance for double charge exchange by allowing the nuclei to perform close collisions with one electron and distant collisions with

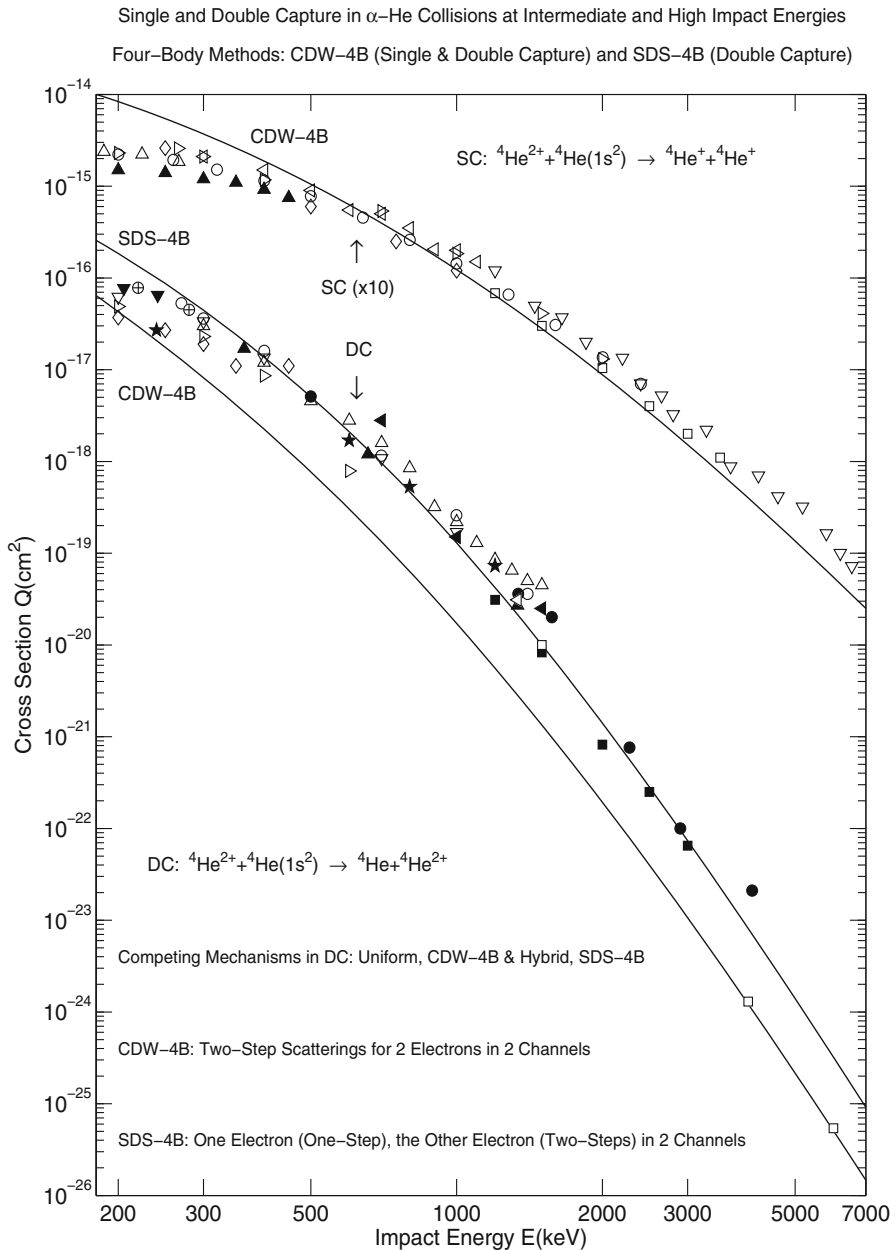


**Fig. 4** Total cross sections  $Q$  ( $\text{cm}^2$ ) versus impact energy  $E$  (keV) for single capture, SC (top), and double capture, DC (bottom), in the  $\alpha$  – He collisions. Theories (the prior form) are for the initial and final ground states. This is the case only in two measurements on DC: Zastrow *et al.* [23] (JET) and Schöffler *et al.* [24] (COLTRIMS). All the remaining measured cross sections on SC and DC are for capture into any final bound state. For the ground-state helium wave functions, the uncorrelated open-shell orbitals ( $1s1s$ ) of Hylleraas [22] are employed in the CDW-4B method (SC, entrance channel) as well as in the SDS-4B and CDW-4B methods (DC, entrance and exit channels). Experimental data: SC (top)  $\blacktriangle$  [25],  $\triangleleft$  [26],  $\nabla$  [40],  $\circ$  [41],  $\triangleright$  [42],  $\square$  [27],  $\triangle$  [43],  $\diamond$  [44]. DC (bottom):  $\diamond$  [25],  $\triangle$  [26],  $\nabla$  [42],  $\blacksquare$  [27],  $\blacktriangle$  [28],  $\blacktriangledown$  [29],  $\blacklozenge$  [30],  $\circ$  [31],  $\blacktriangleleft$  [32],  $\triangleleft$  [33],  $\triangleright$  [34],  $\oplus$  [35],  $\square$  [36],  $\bullet$  [37],  $\boxplus$  [23],  $\star$  [24]. For details, see the main text

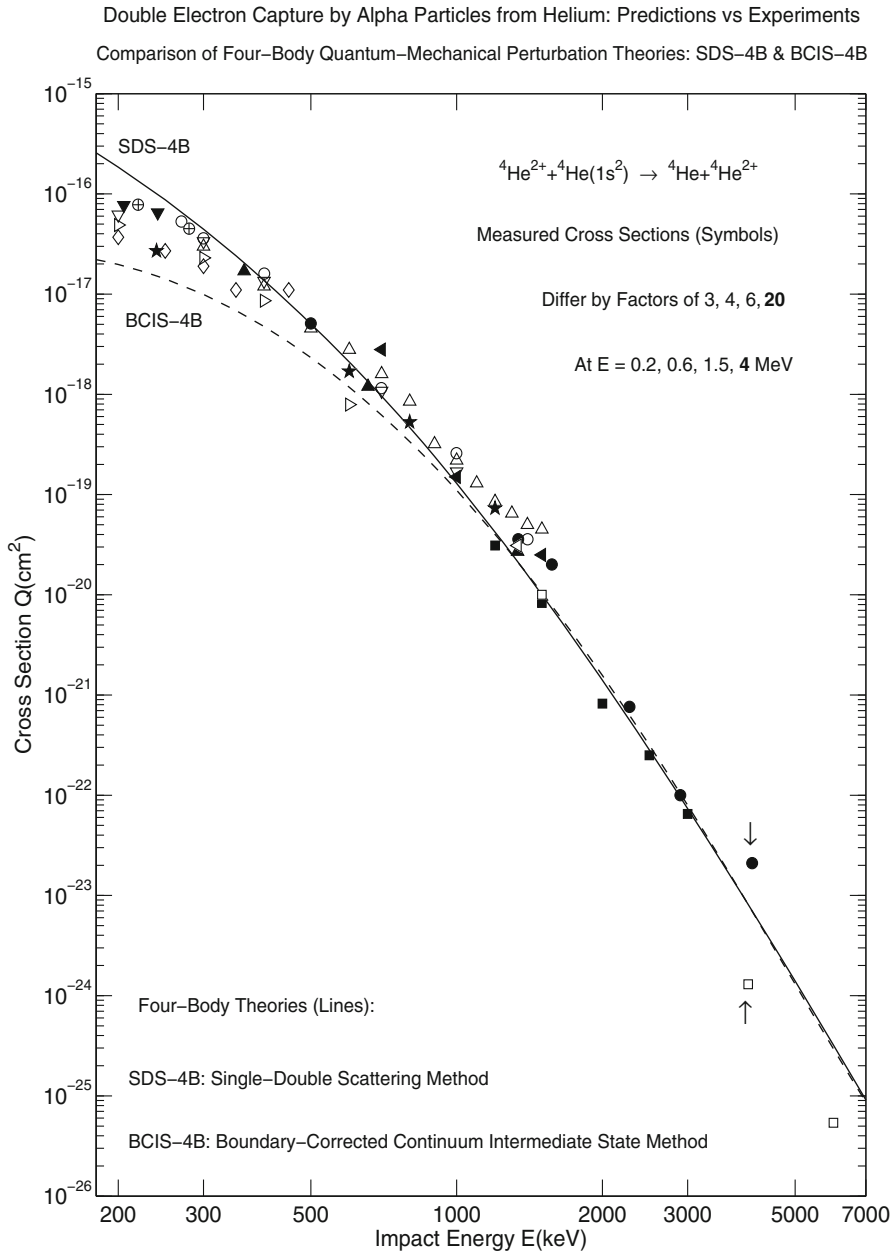


**Fig. 5** Total cross sections  $Q(\text{cm}^2)$  versus impact energy  $E(\text{keV})$  for double capture, DC, in the  $\alpha - \text{He}$  collisions. Theories (the prior form) are for the initial and final ground states of helium. This is the case only in two measurements: Zastrow *et al.* [23] (JET) and Schöffler *et al.* [24] (COLTRIMS). All the remaining measured cross sections are for capture into any final helium bound state. For the ground-state helium wave functions, the theories employ the uncorrelated open-shell orbitals ( $1s1s$ ) of Hylleraas [22] in the entrance and exit channels. Experimental data:  $\diamond$  [25],  $\triangle$  [26],  $\nabla$  [42],  $\blacksquare$  [27],  $\blacktriangle$  [28],  $\blacktriangledown$  [29],  $\blacklozenge$  [30],  $\circ$  [31],  $\blacktriangleleft$  [32],  $\blacktriangleleft$  [33],  $\blacktriangleright$  [34],  $\oplus$  [35],  $\square$  [36],  $\bullet$  [37],  $\boxplus$  [23],  $\star$  [24]. For details, see the main text

the other electron. This flexibility of the SDS-4B method is practical since all the calculations can be performed with the same complexity as in the BCIS-4B and BDW-4B methods. The superiority of the SDS-4B method over the CDW-4B method can be understood by the main mathematical reason, as well. It is the fact that the SDS-4B method is void of the 'multiplication effect' (the product of the two full electronic Coulomb waves per channel), which impedes the performance of the CDW-4B method for DC.

The SDS-4B and BCIS-4B methods for DC are compared in Fig. 5. Herein, the SDS-4B method is seen to be superior to the BCIS-4B method. More specifically, below about 1000 keV, the SDS-4B method is more successful than the BCIS-4B method in predicting the experimental data. Above 1000 keV, the two methods give the cross sections  $Q$  in a very close proximity of each other or even almost coincident. The reason for which the line for  $Q$  in the SDS-4B method lies considerably above that in the BCIS-4B method is in the absence and presence of the Coulomb  $R$ -dependent phase factor in the former and latter theory, respectively.

This phase disappears altogether from the SDS-4B method for  $Z_p = Z_T$  as in process (30). Oscillations (with the underlying destructive interferences) of such a phase reduce  $Q$  in the BCIS-4B method (as discussed with Fig. 2). Conversely, the lack of these oscillations in the SDS-4B method leads to the augmented  $Q$  by an extent sufficient for a visibly improved agreement between the theory and measurements (Fig. 5).

## 4 Conclusions

A class of two-electron rearranging collisions between alpha particles and helium is studied theoretically at intermediate and high impact energies. Addressed are quantum-mechanical four-body distorted wave (DW) perturbative methods on double capture (DC) at 100–8000 keV. A comparative analysis is performed using six DW theories with the correct initial and final boundary conditions (CB1-4B, CDW-4B, CDW-EIS-4B, BCIS-4B, BDW-4B, SDS-4B). The first mentioned method is of the first-order, while the remaining five are of the second-order. A DW method for DC is of the second-order only if it includes at least one electronic full Coulomb wave function for the continuum intermediate states. The CB1-4B method has no such DW functions. In contrast, the CDW-4B method has four electronic full Coulomb waves compared with two such functions in the CDW-EIS-4B, BCIS-4B, BDW-4B and SDS-4B methods.

Taking into account some of continuum states in an intermediate channel should improve the agreement between the DW theories and the measurements. The reason is in the dominance of ionization over capture at higher energies. To include such states, the CDW-4B, CDW-EIS-4B, BCIS-4B and BDW-4B methods for DC consider simultaneous capture of both electrons from their twofold continuum intermediate states in one or two channels. In the SDS-4B method, one electron is first emitted into a continuum state and then captured from that ionization channel, while capture of the other electron occurs directly from a bound state. This sequence of scattering events is symmetrized to allow for the electron exchange effect to take place.

At higher energies, the DW theories can distinguish the two main collisional pathways for DC through single and double scatterings of electrons with nuclei. The former is direct (one step) with no electronic intermediate channels for either electron. The latter is indirect (two steps) with some intermediate ionizing channels for one or both electrons. In single collisions, capture by fast projectile nuclei takes place only for electrons with high longitudinal momentum components in the bound states. However, double collisions can occur with no recourse to large momentum components in the impulse representation of the electronic bound-state wave functions. As such, single and double scatterings can happen in different parts of the configuration space of the four interacting charged particles.

Thus, if both electrons should simultaneously undergo double scatterings in two channels, they necessarily ought to occupy nearly the same spatial positions at almost the same time. This is typical of the CDW-4B method for DC where, at sufficiently high energies, double scattering is manifested especially by the Thomas-like peaks in differential cross sections,  $dQ/d\Omega$ . Such a demanding restriction can partially be lifted by allowing single collisions for one electron and double collisions for the other electron in each channel, as in the SDS-4B method. It is then of interest to assess which of these competing mechanisms might prevail in DC at intermediate and high energies.

The general DW framework is wide open to different choices of distorted waves and distorting potentials, each of which can, in principle, be theoretically well founded as long as the correct boundary conditions are satisfied in the entrance and exit channels. Still, even with the latter conditions duly fulfilled, it becomes a matter of a serious concern if this freedom and flexibility is compromised by potential significant discrepancies among different DW choices.

It is then ultimately the experiment that can help in identifying the most probable mechanism offered by various DW theories. The past applications of such a criterion of proven validity to single capture (SC) and DC in the same heavy particle collisions met with unequal success. For total cross sections  $Q$  in SC, above the Massey peak area of impact energy  $E$  (around 100 keV/amu and up to several MeV/amu), the available measurements systematically confirmed a robust reliability of several DW theories that gave similar results despite very different choices of distorted waves.

However, a similar performance is generally unmatched by DC for which various DW selections yield vastly different cross sections  $Q$ . This occurs at the same mentioned energies  $E$ , i.e. well within the anticipated validity domain of the DW theories. Nevertheless, the existing experimental data can discriminate between the two types of these DW theories. One type of the DW methods assumes 'the concerted or uni-mode' for DC by requiring that both electrons are simultaneously transferred by way of an identical mechanism per channel (single or double collisions or both). These are the CB1-4B, CDW-4B, CDW-EIS-4B, BCIS-4B and BDW-4B methods. They do not mix single with double scattering mechanisms in the given channel. However, none of these theories can successfully represent the mutually concordant measured cross sections from different experiments at all the energies above 200 keV for DC in the  $\alpha - \text{He}$  collisions.

The other type of the DW theories adopts a symmetrized, twofold mechanism. It explicitly combines the two 'individual or separate modes' for DC in each channel

by hybridizing a single scattering for one electron and a double scattering for the other electron. As per its very name, the single-double scattering method, the SDS-4B method, is an example of this alternative mechanism for DC. It reproduces excellently most of the measured cross sections at  $E \geq 200$  keV for the  $\alpha - \text{He}$  collisions. The implication is that DC becomes more likely with the coupled single-double scatterings in each channel than with two double scatterings in both channels. The conclusion is that the adequacy of the SDS-4B method for DC is comparable to the established reliability of the CDW-4B method for SC in the same  $\alpha - \text{He}$  collisions above 200 keV. This achievement restores confidence in the lowest-order of the Dodd-Greider perturbation series for DC. Such a platform enables affordable comprehensive numerical computations on  $Q$  also for DC in various applications, not only within ion-atom collision physics, but likewise in several neighboring branches and disciplines of scientific research.

**Acknowledgements** The Author thanks the Radiumhemmet Research Fund at the Karolinska University Hospital as well as the Fund for Research, Development and Education (FoUU) of the Stockholm County Council.

**Author contributions** The Author himself designed and performed all the work in this study.

**Funding** Open access funding provided by Karolinska Institute. This work is funded by the Radiumhemmet Research Funds, King Gustaf the Fifth Jubilee Fund at the Karolinska University Hospital, Fund for Research, Development and Education of the Stockholm County Council.

**Data Availability Statement** Data from this work can be made available to other researchers in this field upon request to the Author.

## Declarations

**Conflicts of interest** The Author declares that he has no known competing funding, employment, financial or non-financial interests that could have appeared to influence the work reported in this paper.

**Open Access** This article is licensed under a Creative Commons Attribution 4.0 International License, which permits use, sharing, adaptation, distribution and reproduction in any medium or format, as long as you give appropriate credit to the original author(s) and the source, provide a link to the Creative Commons licence, and indicate if changes were made. The images or other third party material in this article are included in the article's Creative Commons licence, unless indicated otherwise in a credit line to the material. If material is not included in the article's Creative Commons licence and your intended use is not permitted by statutory regulation or exceeds the permitted use, you will need to obtain permission directly from the copyright holder. To view a copy of this licence, visit <http://creativecommons.org/licenses/by/4.0/>.

## References

1. L.R. Dodd, K.R. Greider, Rigorous solution of three-body scattering processes in the distorted-wave formalism. *Phys. Rev.* **146**, 675–686 (1966)
2. Dž. Belkić, R. Gayet, A. Salin, Electron capture in high-energy ion-atom collisions. *Phys. Rep.* **56**, 279–369 (1979)
3. F. Busnengo, A.E. Martínez, R.D. Rivarola, Single electron capture from He targets. *J. Phys. B* **29**, 4193–4205 (1996)



4. L. Gulyás, P.D. Fainstein, T. Shirai, Extended description for electron capture in ion-atom collisions: Application of model potentials within the framework of the continuum distorted wave theory. *Phys. Rev. A* **65**, 052720 (2002)
5. Dž. Belkić, *Principle of Quantum Scattering Theory* (Taylor & Francis, London, 2004)
6. D. Delibašić, N. Milojević, I. Mančev, Dž. Belkić, Electron removal from hydrogen atoms by impact of multiply charged nuclei. *Eur. Phys. J. D* **75**, 115 (2021)
7. D. Delibašić, N. Milojević, I. Mančev, Dž. Belkić, Electron transfer from atomic hydrogen to multiply-charged nuclei at intermediate and high energies. *At. Data Nucl. Data Tables* **139**, 101417 (2021)
8. N. Milojević, I. Mančev, D. Delibašić, Dž. Belkić, Cross sections for single-electron capture from heliumlike targets by fast nuclei. *Phys. Rev. A* **107**, 052806 (2023)
9. Dž. Belkić, Symmetric double charge exchange in fast collisions of bare nuclei with helium-like atomic systems. *Phys. Rev. A* **47**, 189-200 (1993)
10. Dž. Belkić, Two-electron capture from helium-like atomic systems by completely stripped projectiles. *J. Phys. B* **26**, 497-508 (1993)
11. Dž. Belkić, I. Mančev, Formation of  $H^-$  by double charge exchange in fast proton-helium collisions. *Phys. Scr.* **45**, 35-42 (1992)
12. Dž. Belkić, I. Mančev, Four-body CDW approximation: Dependence of prior and post total cross sections for double charge exchange upon bound-state wave-functions. *Phys. Scr.* **46**, 18-23 (1993)
13. Dž. Belkić, Importance of intermediate ionization continua for double charge exchange at high energies. *Phys. Rev. A* **47**, 3824-3844 (1993)
14. Dž. Belkić, Double charge exchange at high impact energies. *Nucl. Instrum. Meth. Phys. Res. B* **86**, 62-81 (1994)
15. Dž. Belkić, I. Mančev, M. Mudrinić, Two-electron capture from helium by fast alpha particles. *Phys. Rev. A* **49**, 3646-3658 (1994)
16. R. Gayet, J. Hanssen, A. Martínez, R. Rivarola, Status of two-electron processes in ion-atom collisions at intermediate and high impact energies. *Comments Atom. Mol. Phys.* **30**, 231–248 (1994)
17. A.E. Martínez, R.D. Rivarola, R. Gayet, J. Hanssen, Double electron capture theories: Second order contributions. *Phys. Scr.* **T80**, 124–127 (1999)
18. Dž. Belkić, Distorted wave theories with correct boundary conditions for double charge exchange in ion-atom collisions at intermediate and high energies. *Adv. Quantum Chem.* **86**, 223-296 (2022)
19. Dž. Belkić, Total cross sections in five methods for two-electron capture by alpha particles from helium: CDW-4B, BDW-4B, BCIS-4B, CDW-EIS-4B and CB1-4B. *J. Math. Chem.* **58**, 1133-1176 (2020)
20. Dž. Belkić, High-energy two-electron transfer in ion-atom collision. *J. Math. Chem.* **61**, 177-184 (2023)
21. Dž. Belkić, R. Gayet, J. Hanssen, I. Mančev, A. Nuñez, Dynamic electron correlations in single capture from helium by fast protons. *Phys. Rev. A* **56**, 3675-3681 (1997)
22. E.A. Hylleraas, Neue Berechnung der Energie des Heliums im Grundzustande, sowie tiefsten Terms von Ortho-Helium. *Z. Phys.* **54**, 347–366 (1929)
23. K.-D. Zastrow, M. O'Mullane, M. Brix, C. Giroud, A.G. Meigs, M. Proschek, H.P. Summers, Double charge exchange from helium neutral beams in a tokamak plasma. *Plasma Phys. Control. Fusion* **45**, 1747–1756 (2003)
24. M.S. Schöffler, J. Titze, LPh.H. Schmidt, T. Jahnke, N. Neumann, O. Jagutzki, H. Schmidt-Böcking, R. Dörner, I. Mančev, State-selective differential cross sections for single and double electron capture in  $He^{+,2+} - He$  and  $p - He$  collisions. *Phys. Rev. A* **79**, 064701 (2009)
25. S.K. Allison, Experimental results on charge-changing collisions of hydrogen and helium atoms and ions at kinetic energies above 0.2 keV. *Rev. Mod. Phys.* **30**, 1137-1168 (1958)
26. L.I. Pivovarov, M.T. Novikov, V.M. Tubaev, Electron capture by helium ions in various gases in the 300-1500 keV energy range. *J. Exp. Theor. Phys. JETP* **15**, 1035-1039 (1962) [*Zh. Eksp. Teor. Fiz.* **42**, 1490-1494 (1962)]
27. N.V. de Castro Faria, F.L. Freire Jr, A.G. de Pinho, Electron loss and capture by fast helium ions in noble gases. *Phys. Rev. A* **37**, 280-283 (1988)
28. V.S. Nikolaev, L.N. Fateeva, I.S. Dmitriev, Ya.A. Teplova, Capture of several electrons by fast multi-charged ions. *J. Exp. Theor. Phys. JETP* **14**, 67-74 (1962) [*Zh. Eksp. Teor. Fiz.* **41**, 89-99 (1961)]
29. K.H. Berkner, R.V. Pyle, J.W. Stearns, J.C. Warren, Single- and double-electron capture by 7.2 to 181 keV  $^3He^{++}$  ions in He. *Phys. Rev.* **166**, 44-46 (1968)
30. J.E. Bayfield, G.A. Khayrallah, Electron transfer in keV-energy  $^4He^{++}$  atomic collisions: I. Single and double electron transfer with He, Ar,  $H_2$  and  $N_2$ . *Phys. Rev. A* **11**, 920-929 (1975)

31. E.W. McDaniel, M.R. Flannery, H.W. Ellis, F.L. Eisele, W. Pope, T.G. Roberts, Compilation of data relevant to rare-gas and rare-gas-monohalide excimer lasers. *US Army Missile Research and Development Command, Redstone Arsenal, Alabama, Vol. I, Technical Report, No. H-78-1* (1977)
32. A. Itoh, M. Asari, F. Fukuzawa, Charge-changing collisions of 0.7–2.0 MeV helium beams in various gases. I. Electron capture. *J. Phys. Soc. Japan* **48**, 943–950 (1980)
33. I.S. Dmitriev, N.F. Vorob'ev, Zh.M. Konovalova, V.S. Nikolaev, V.N. Novozhilova, Ya.A. Teplova, Yu.A. Faĭnberg, Loss and capture of electrons by fast ions and atoms of helium in various media. *J. Exp. Theor. Phys. JETP* **57**, 1157–1164 (1983) [*Zh. Eksp. Teor. Fiz.* **84**, 1987–2000 (1983)]
34. M.E. Rudd, T.V. Goffe, A. Itoh, Ionization cross sections for 10–300-keV/amu and electron-capture cross sections for 50–150-keV/u  $^3\text{He}^{2+}$  ions in gases. *Phys. Rev. A* **32**, 2128–2133 (1985)
35. R.D. DuBois, Ionization and charge transfer in  $\text{He}^{2+}$ -rare gas collisions. *Phys. Rev. A* **33**, 1595–1601 (1986)
36. R. Schuch, E. Justiniano, H. Vogt, G. Deco, N. Grün, Double electron capture by  $\text{He}^{2+}$  from He at high velocity. *J. Phys. B* **24**, L133–L138 (1991)
37. V.V. Afrosimov, D.F. Barash, A.A. BasalaeV, N.A. Gushchina, K.O. Lozhkin, V.K. Nikulin, M.N. Panov, I.Yu. Stepanov, Single- and double-electron capture from many-electron atoms by  $\alpha$  particles in the MeV energy range. *J. Exp. Theor. Phys. JETP* **77**, 554–561 (1993) [*Zh. Eksp. Teor. Fiz.* **104**, 3297–3310 (1993)]
38. R. Dörner, V. Mergel, L. Spielberger, O. Jagutzki, H. Schmidt-Böcking, J. Ullrich, State-selective differential cross sections for double-electron capture in 0.25–0.75-MeV  $\text{He}^{2+}$  – He collisions. *Phys. Rev. A* **57**, 312–317 (1998)
39. J. Silverman, O. Platas, F.A. Matsen, A discussion of analytic and Hartree-Fock wave functions for  $1s^2$  configurations from  $\text{H}^-$  to C. *J. Chem. Phys.* **32**, 1402–1406 (1960)
40. P. Hvelplund, J. Heinemeier, E. Horsdal-Pedersen, F.R. Simpson, Electron capture by  $\text{He}^{2+}$  ions in gases. *J. Phys. B* **9**, 491–496 (1976)
41. M.B. Shah, H.B. Gilbody, Single and double ionisation of helium by  $\text{H}^+$ ,  $\text{He}^{2+}$  and  $\text{Li}^{3+}$ . *J. Phys. B* **18**, 899–914 (1985)
42. R.D. DuBois, Ionization and charge transfer in  $\text{He}^{2+}$  – rare gas collisions. II. *Phys. Rev. A* **36**, 2585–2593 (1987)
43. M.B. Shah, P. McCallion, H.B. Gilbody, Electron capture and ionisation in collisions of slow  $\text{H}^+$  and  $\text{He}^{2+}$  ions with helium. *J. Phys. B* **22**, 3037–3046 (1989)
44. V. Mergel, R. Dörner, J. Ullrich, O. Jagutzki, S. Lencinas, S. Nüttgens, L. Spielberger, M. Unverzagt, C.L. Cocke, R.E. Olson, M. Schulz, U. Buck, H. Schmidt-Böcking,  $\text{He}^{2+}$  on He: State-selective, scattering-angle dependent capture cross sections measured by cold target recoil ion momentum spectroscopy (COLTRIMS). *Nucl. Instrum. Meth. Phys. Res. B* **98**, 593–596 (1995)
45. H. Schmidt-Böcking, J. Ullrich, R. Dörner, C.L. Cocke, The COLTRIMS reaction microscope - the spyhole into the ultrafast entangled dynamics of atomic and molecular system. *Ann. Phys. (Berlin)* **533**, 2100134 (2021)
46. Dž. Belkić, A quantum theory of ionisation in fast collisions between ions and atomic systems. *J. Phys. B* **11**, 3529–3552 (1978)
47. D.S.F. Crothers, J.F. McCann, Ionisation of atoms by ion impact. *J. Phys. B* **16**, 3229–3242 (1983)
48. Dž. Belkić, Electron detachment from the negative hydrogen ion by proton impact. *J. Phys. B*, **30**, 1731–1745 (1997)
49. Dž. Belkić, Review of theories on ionization in fast ion-atom collisions with prospects for applications to hadron therapy. *J. Math. Chem.* **47**, 1366–1419 (2010)
50. F. Melchert, S. Krüdener, K. Huber, E. Salzborn, Electron detachment in  $\text{H}^+ - \text{H}^-$  collisions. *J. Phys. B* **32**, L139–L144 (1999)
51. A.E. Martínez, G.R. Deco, R.D. Rivarola, P.D. Fainstein, K-shell vacancy production in asymmetric collisions. *Nucl. Instrum. Meth. Phys. Res. B* **34**, 32–36 (1988)
52. J.H. McGuire, Multiple-electron excitation, ionization and transfer in high-velocity atomic and molecular collisions. *Adv. At. Mol. Phys.* **29**, 217–323 (1992)